Am J Cancer Res 2021;11(6):3271-3284
www.ajcr.us /ISSN:2156-6976/ajcr0133198

Original Article

Inhibition of P53-mediated cell cycle control as the determinant in dedifferentiated liposarcomas development

Mossane Stocker[1,2], Louis-Romée Le Nail[3], Hubert De Belenet[2], Jay S Wunder[4], Irene L Andrulis[4], Nalan Gokgoz[4], Nicolas Levy[1,5], Jean-Camille Mattei[1,5*], Sylviane Olschwang[1,2*]

[1]INSERM UMR1251 Marseille Medical Genetics Genetics, Marseille, France; [2]GCS Pour l'Enseignement et la Recherche, Ramsay Santé, Hôpital Privé Clairval, Marseille, France; [3]CHRU Trousseau, Tours, France; [4]Lunenfeld_Tanenbaum Research Institute, University of Toronto, Toronto, Canada; [5]AP-HM, Marseille, France. [*]Equal contributors.

Received March 16, 2021; Accepted April 28, 2021; Epub June 15, 2021; Published June 30, 2021

Abstract: Liposarcomas are a heterogeneous group of sarcomas, including well-differentiated and dedifferentiated liposarcoma, myxoid/round cell liposarcoma, and pleomorphic liposarcoma. Complete surgical resection is the key of treatment. Radiotherapy, based on the tumor grade and the vicinity of critical structures with the tumor, can be used to prevent local recurrence. The group of dedifferentiated liposarcomas (DDLS) is poorly sensitive to adjuvant chemotherapy. Improved understanding of the genetic aberrations that lead to liposarcoma initiation is necessary for the development of targeted therapies to improve tumor control and survival. DDLS share genetic abnormalities with other groups, exhibiting high-level amplifications of chromosome 12, including the *MDM2* and *CDK4* genes, and harbor additional amplifications of chromosomes 6 and 1. Novel therapies targeted at the gene products of chromosome 12 are currently considered in clinical trials. Our work consisted in a genomic characterization of DDLS to draw up a complete picture of alterations, including genomic signatures, tumor mutation burden, gene mutations, copy number variations, translocations, gene fusions and methylation modifications. Analysis of translocations helped to understand the mechanisms underlying the amplification processes. Combination of mutations and loss of heterozygosity or homozygous deletions were detected and led to inactivate tumor suppressor genes (TSG). In contrast, methylation anomalies seemed not linked to any particular genomic profile. All identified anomalies, whether amplifications and/or TSG inactivation, involve genes playing a role in p53 regulation, that appears to be the epicenter of the initiation process in DDLS tumorigenesis, as is also known to be responsible for Li-Fraumeni syndrome, a family cancer syndrome highly predisposing to sarcomas.

Keywords: Dedifferentiated liposarcoma, p53 pathway, genetic profile, targeted therapy

Introduction

Sarcomas are rare malignant tumors that expand from mesenchymal tissues. Liposarcomas (LS) are usually characterized by adipocytic differentiation. This is the most common histologic type of soft tissue sarcomas in adults (25%) [1, 2]. The incidence is approximately 1/100,000 people/year [3]. They affect all age groups but most frequently occur in adults sixty years of age and older and involve limbs, peritoneal region or more rarely mediastinum [4, 5].

Cytogenetics and molecular features distinguish five different subtypes of liposarcomas, used for diagnostic and therapeutic management [6]. Well-differentiated liposarcomas (WDLS) and dedifferentiated liposarcomas (DDLS) represent the most common group (approximately 80%). DDLS is defined by the association of a well-differentiated liposarcoma component and undifferentiated component which is most often dense or pleomorphic, or more rarely of a heterologous nature such as rhabdomyosarcoma or leiomyosarcoma. LS harbor common chromosomal alterations (supernumerary and giant chromosomes) with amplification of the 12q14-15 region including the *MDM2* gene, often associated with copy number change the *SAS*, *CDK4* and *HMGA2* genes.

This *MDM2* amplification can be highlighted by immunostaining and/or FISH analysis and is considered a diagnostic criterion of LS. In case of remaining doubt about the underlying diagnosis, amplification of the chromosomal region 12q14.15 and possibly 1p32 or 6q23 provides definitive evidence [2].

More recently, Hirata et al. proposed dividing DDLS into three subgroups according to copy number variations (CNV) which identified distinct differences in the rates of disease-specific survival and progression-free survival. One group includes amplification of both 12q15 and 1p32.1 regions, and the second group amplification of the 12q15 region only. The smallest third group is more heterogeneous and exhibits chromosomal gains or losses mainly associated with TP53 and PI3K-AKT signaling [7, 8].

DDLS have a high risk of local recurrence (40 to 60% depending on their anatomic location, size and grade) sometimes leading to unresectability, especially in the retroperitoneum. The metastatic risk in LP is 15-25%. But largely depends on the tumor subtype. The 5-year survival is approximately 100% in WDLS (87% at 10 years), 88% in myxoid sarcomas (76% at 10 years), 56% in pleomorphic liposarcomas (39% at 10 years) [9] and around 60% at 5 years (40% at 10 years) in DDLS [10, 11].

The therapeutic approach to management of patients with LP is quite limited, and little progress has been made to improve overall survival or recurrence risk over the past few decades. When possible, the mainstay of treatment is based on complete but sometimes complex surgical resection. Indeed, the tumor can invade critical structures such as vessels or nerves or organs, often limiting the completeness of surgical resection or leading to major morbidity for patients. Surgery is usually supplemented by adjuvant chemotherapy and/or radiotherapy to improve resectability and minimize local tumor relapse. Active research is ongoing to identify new therapeutic targets based on specific and recurrent genomic anomalies to improve tumor control and survival. The most recent studies focused on overexpressed genes or proteins [12] but are limited by intratumor heterogeneity and diversity of genomic profiles [9, 13, 14]. Targeted therapy mainly includes antagonists of MDM2 and CDK4; PPARγ ligand agonists are known to induce normal differentiation of preadipocytes in human liposarcoma cells with reduced immunohistochemical expression of the proliferation marker Ki-67. Trabectedin and PI3K inhibitors are relevant in myxoid liposarcoma [15]. Selinexor, a selective exportin 1 inhibitor, has shown promising in a phase I trial in advanced cancer patients with confirmed disease progression, including 19 with DDLS [16].

Recently, cancer research explored epigenetics. As DNA methylation plays an important role in the regulation of expression and tissue-specificity, the challenge is now to understand the related mechanisms in tumorigenesis as random occurrence, environmental pressure response or direct consequence of oncogenic rearrangement [17]. It has been shown that large disruption of DNA methylation profiles plays a role in accumulation of genetic mutations [18]. As an example, regions of several hypomethylated megabases have been identified in colon and breast cancer cells [19, 20]. It has been suggested that these epigenetic anomalies might also be related to the aggressiveness. These observations let consider new therapeutic approaches. In sarcomas, the identification of target genes for a specific regulatory process in Ewing's sarcoma indirectly led to the development of targeted treatments [21]. It would therefore be interesting to document this phenomenon in LS, as it was previously explored in other sarcomas [22, 23].

The aim of our study was to characterize and combine the complete genetic and epigenetic profiles of human DDLS in order to identify potential therapeutic targets. We based our study on identifying mutations, CNV, translocations and methylation profiles specific to the tumor cells, then questioning if possible common altered pathways exist in this subtype of liposarcomas.

Material and methods

Material

The project was registered as a clinical research study in the French dedicated agency ANSM (Agence Nationale de la Sécurité du Médicament) under no. RCB 2017-A02547-46 as ongoing care. It was registered with a favorable recommendation by the people protection committee CPP Ile de France 1 on 01/18/2018

under no. 2017-oct-14683ND. All participants signed an informed consent document.

The project included 10 patients affected by dedifferentiated liposarcoma confirmed by histological and molecular diagnosis and treated by primary surgery. None of these sarcoma patients received preoperative radiation or chemotherapy so the tumor specimens harvested for molecular analysis were treatment-naïve. Ten control patients were selected based on age, gender and tumor location. Patients were enrolled in from the surgery departments of Trousseau Hospital (Centre Hospitalier Régional Universitaire de Tours, France) and «Sinaï Health System» (Mount Sinaï hospital and the Lunenfeld-Tanenbaum Research Institute, Toronto, Canada). Control patients were selected from Residence du Parc (Marseille, France) and AP-HM Hôpital Nord (Marseille, France) hospitals, where they were admitted for prosthetic surgery on the hip, knee or shoulder for arthrosis.

No supplementary intervention was added to the standard procedures in the present study.

In addition to the usual inclusion and non-inclusion criteria applied for clinical research projects on adults, inclusions were not restrained to a specific gender but needed a complete clinical examination. Non-inclusion was applied if chronic inflammatory disease or previous personal cancer history.

For each case, tumor and adjacent but distant (non-inflammatory) normal fat tissues were selected at time of wide-resection surgery. Samples were stored in 2 mL of stabilization solution for nucleic acids Allprotect® Tissue Reagent (Qiagen®, France) then frozen at -80°C. Fat tissue was stored using the same conditions for controls.

Methods

Nucleic acids preparation

DNA and RNA were extracted from tissue samples using purification AllPrep DNA/RNA and RNeasy Lipid Tissue (Qiagen®, France) depending on the lipid content. Fragment Analyzer™ (Agilent, France) was used for quantification.

Targeted exome sequencing

Library preparation, exome capture, sequencing and data analysis were performed by IntegraGen SA (Evry, France). Genomic DNA was captured using Twist Human Core Exome Enrichment System (Twist Bioscience) and IntegraGen Custom, according to Gnirke et al. [24]. Sequence capture, enrichment and elution were performed according to the manufacturer's instruction and protocols (Twist Bioscience, USA) without modification except for library preparation performed with NEBNext® Ultra II kit (New England Biolabs, Evry, France). For library preparation 150 ng of each genomic DNA were fragmented by sonication and purified to yield fragments of 150-200 bp. Paired-end adaptor oligonucleotides from the NEB kit were ligated on repaired, a-tailed fragments then purified and enriched by 7 PCR cycles. 500 ng of these purified libraries were then hybridized to the Twist oligo probe capture library for 16 hours in a singleplex reaction. After hybridization, washing, and elution, the eluted fraction was PCR-amplified with 8 cycles, purified and quantified by QPCR to obtain sufficient DNA templates for downstream applications. Each eluted-enriched DNA sample was then sequenced on a NovaSeq (Illumina, Evry, France) as paired-end 100 reads. Image analysis and base calling was performed using Illumina Real Time Analysis with default parameters.

RNA sequencing

Libraries were prepared with NEBNext Ultra II Directional RNA Library Prep Kit for Illumina protocol according the supplier's recommendations. Briefly the key stages of this protocol were successively the purification of PolyA containing mRNA molecules using poly-T oligo attached magnetic beads from 1 µg total RNA (with the Magnetic mRNA Isolation Kit from NEB), a fragmentation using divalent cations under elevated temperature to obtain approximately 300-bp pieces, double-strand cDNA synthesis and finally Illumina adapters ligation and cDNA library amplification by PCR for sequencing. Sequencing was then carried out on paired end 100-b reads of Illumina NovaSeq. Image analysis and base calling was performed using Illumina Real Time Analysis (v3.4.4) with default parameters.

Methylome analysis

Methylomes were characterized on Infinium™ «Methylation EPIC™» 850K (Illumina, Evry, France) chips by IntegraGen SA (Evry, France).

Bioinformatics analyses

DNA and RNA analyses were processed using the Mercury application (IntegraGen Genomics). Comparisons of genomic profiles between external controls, internal controls and cases have been conducted. Germline and acquired mutations have been registered, as well as copy number variations (amplifications and deletions/losses of heterozygosity). RNA analyses were used to detect translocations. Methylome analysis was driven by GeCo staff (Integragen, France). Briefly principal component analysis (PCA), hierarchical clustering and consensus clustering were applied to classify samples according to their genome-wide methylation pattern. All analyses were conducted in R statistical software.

Mutations and CNV detection

Sequence reads were mapped to the Human genome build (hg38) by using the Burrows-Wheeler Aligner (BWA) tool. The duplicate reads (e.g., paired-end reads in which the insert DNA molecules have identical start and end locations in the Human genome) were removed (sambamba tools). Variant calling for the identification of SNVs (Single Nucleotide Variations) and small insertions/deletions (up to 20bp) were performed via the Broad Institute's GATK Haplotype Caller GVCF tool (GATK3.8.1) for constitutional DNA and via the Broad Institute's MuTect tool (2.0, -- max_alt_alleles_in_normal_count = 2; -- max_alt_allele_in_normal_fraction = 0.04) for somatic DNA. A Fisher's Exact Test was applied after MuTect2 variant calling to improve filtering of variants with strand bias. The panel of normal (PON) is a type of resource which used in somatic variant analysis when no normal is available. To create this PON, we used constitutional sample captured (Agilent and Twist Technologies) and sequenced at Integragen and in addition, the PON of Broad Institute. An in-house post-processing to filter out candidate somatic mutations that are more consistent with artifacts or germline mutations was applied. Only the somatic mutations considered as PASS or t_lod_fstar were retained, and a somatic score of at least 1 was added with analysis without PON. The somatic score was calculated for each mutation ranging from 1 to 30, with a score of 30 translating to the highest confidence index. This score takes into account counts and the frequencies of mutated alleles in both samples to minimize false positive variations. Finally, mutations with a QSS score below 20 and a VAF of tumor < 0.02 were removed. An additional variant caller besides MuTect2 was used to rescue erroneously filtered variants. More precisely, we run VarScan2 on somatic variants indicated as clustered_ events by Mutect2 and checked if any high confidence variants were also identified (but subsequently filtered) by MuTect2. Ensembl's VEP (Variant Effect Predictor, release VEP95.1) program processes variants for further annotation. This tool annotates variants, determines the effect on relevant transcripts and proteins, and predicts the functional consequences of variants. It takes into account data available in the gnomAD, the 1000 Genomes Project and the Kaviar databases. Moreover, an in-house database enables to filter out sequencing artefacts.

Five bioinformatics algorithms for pathogenicity are available to predict the functional, molecular and phenotypic consequences of coding and non-coding SNPs. This includes DANN, FATHMM, MutationTaster, SIFT and Polyphen. The clinical and pathological significance from the ClinVar database was added. Other information, including quality score, homozygote/heterozygote status, count of variant allele reads, and presence of the variant in the COSMIC database were reported. RegulomeDB is used to annotate SNPs in known and predicted regulatory elements in the intergenic regions.

Bioconductor DNACopy package was used to investigate genomic copy number aberrations (CNA) (e.g., copy number gains and copy number losses), by comparing the normal DNA exome data to a reference sample pool. It implements the circular binary segmentation (CBS) algorithm to segment DNA copy number data. All changes are annotated with the catalog of the Database of Genomic Variants (DGV) to provide a comprehensive summary of structural variation in the human genome. Bioconductor DNACopy package was used to investigate B-allele frequency (BAF) with SNPs with a frequency of more than 0.1 in 1000 Genomes Project. It implements the circular binary segmentation (CBS) algorithm to segment BAF data. The Advanta™ Sample ID Genotyping Panel is a 96-SNP assay enabling laboratories to generate a sample-specific genetic finger-

print in order to confirm the identity between the results delivered and the DNA sample received. This genetic fingerprint includes 10 quality assessment SNPs, 6 gender SNPs, 80 exonic SNPs. At the end of the bioinformatics process, the genotyping results of the DNA sample received were compared against the sequencing data and a concordance score was calculated. This enables detection of failures in the sample preparation process (contamination, sample inversion, etc.) and ensures the concordance between the samples received and the results delivered.

Mutational load

The mutational load was calculated by dividing the number of somatic mutations by the number of bases having a depth greater than 10. The data come from the article Mutational heterogeneity in cancer and the search for new cancer genes [25]. "Somatic mutation frequencies observed in exomes from 3,083 tumor-normal pairs are plotted. Each dot corresponds to a tumor-normal pair, with vertical position indicating the total frequency of somatic mutations in the exome. Tumor types are ordered by their median somatic mutation frequency, with the lowest frequencies (left) found in hematological and pediatric tumors, and the highest (right) in tumors induced by carcinogens such as tobacco smoke and UV light". The somatic mutations used for the mutational load were filtered as follows: Somatic score > 3, FILTER = PASS, Mutated Allele Frequency in Tumor tissue ≥ 5%, Mutated Allele Count in Tumor tissue ≥ 3, Mutated Allele Frequency in Constitutional tissue < 4%, Integragen het freq ≤ 1%, Integragen heterozygous frequency ≤ 1%, Integragen homozygous frequency ≤ 1% and EVS & 100G & Exac variant frequency ≤ 0.5% and consequences on protein: Stop, Start, Missense, Splice for the SNPs and Inframe, Frameshift for the indels.

Microsatellite analysis

The MSIsensor software with default filters was used to detect variants in microsatellite regions and annotate them as germline or somatic. The microsatellite instability threshold is 3.5% (11% in the case of PON analysis) according to Beifang Niu et al. [26].

Mutational signature

Mutational signatures are displayed on the basis of the trinucleotide frequency of the human genome [27]. Asterisk indicates mutation type exceeding 20%. The somatic mutations used for the signature were filtered as follows: Somatic score > 3, FILTER = PASS, Mutated Allele Frequency in Tumor tissue ≥ 5%, Mutated Allele Count in Tumor tissue ≥ 3, Mutated Allele Frequency in Constitutional tissue < 4%, Integragen heterozygous frequency ≤ 1%, Integragen homozygous frequency ≤ 1% and EVS & 100G & Exac variant frequency ≤ 0.5%.

Methylation level

Methylation levels (beta-values) and statistics were exported with Genome Studio software. Data points with a detection *p*-value > 0.05 were masked. We filtered out all positions with a common polymorphism (minor allele frequency > 0.05) less than 2 bases away from the CpG or a detection *p*-value > 0.05 for more than 20% of samples.

Signal integration by feature

Methylation rates were integrated across CpG island (CGI)-based and gene-based features using custom scripts. CGI-based features were defined as follows: CpG islands (from UCSC database hg19/GRCh37), shores (2 kb on each side of the island) and shelves (2 Kb outside the shores). Gene-based features were defined based on Ensembl *homo sapiens* GRCh37.p13 assembly. We calculated for each gene the methylation rate across the promoter region (TSS ± 500 bp) and the gene body.

Unsupervised classification

We selected the 5000 most variant autosomal CpG sites (based on standard deviation of beta-values) to perform principal component analysis (PCA), hierarchical clustering and consensus clustering to classify samples according to their genome-wide methylation pattern. All analyses were conducted in R statistical software. We used standard R functions to perform the PCA and hierarchical clustering (with Euclidean distance and Ward method). We used consensus clustering (Bioconductor *ConsensusClusterPlus* package) to examine the stability of the clusters.

Table 1. Demographic characteristics of DDLS patients and external controls

DDLP case	Gender	Age	Tumor localization	External control	Age	Localization
1T	M	66	deltoid	2	65	shoulder
2T	F	48	proximal thigh	6	45	lower limb
3T	M	59	calf	3	52	lower limb
4T	M	70	distal psoas	5	66	lower limb
5T	M	68	left forearm	1	67	upper limb
6T	F	65	right posterior thigh	9	71	lower limb
7T	F	62	left thigh	8	64	lower limb
8T	M	69	right hip	10	64	lower limb
9T	M	74	proximal thigh	7	80	lower limb
10T	M	72	left thigh	4	68	hip

Differential methylation analysis

We only tested positions with a minimum detection *p*-value below 0.01 to improve the statistical power of the analysis. We used a Wilcoxon test to assess for differential methylation. *P*-values were corrected for multiple testing using Benjamini-Hochberg procedure. We applied a q-value threshold of ≤ 0.05 (0.25 for paired samples) and a minimum delta fold change of 0.05 to define differentially methylated positions. Gene-based and CGI-based segmentation of the data was done as in "signal integration by feature" analysis.

Pathway enrichment analysis

We used hypergeometric tests to identify gene sets from the MSigDB v7.0 database overrepresented among the lists of up- or down-regulated genes, correcting for multiple testing with the Benjamini-Hochberg procedure.

Results

Samples

Cases were defined as tumor samples resected from 10 DDLS patients, and each was paired to an adjacent but distant sample of fat tissue which served as an internal control, as well as normal fat tissue from patients undergoing prosthetic surgery for arthrosis which served as external controls, with matching based on gender, age (± 6 years), and anatomic tumor location (**Table 1**). Good quality and sufficient amount of DNA was obtained for all samples, but only 6 RNAs were suitable for transcriptomic analysis. Exomic and adjacent splicing regions of germline and tumor DNA samples were captured then paired-end sequenced at 50× and tumor DNA at 250× depth respectively with a coverage higher than 98%; mRNAs were captured, and 40.10^6 paired-end sequences were generated.

Mutations analysis

Tumor signatures, mutational burden (TMB) and single nucleotide variants (SNV) are listed in **Table 2**. Three signatures were observed: 1 in all cases but 6T; in addition, cases 2T, 4T and 6T harbored signature 15, and 2T also displayed signature 6. TMB ranged from 0,11 to 1,48 mutations per megabase. A total of 14 SNV with a variation allelic fraction (VAF) from 3 to 81% were retained, including 9 of functional class-4 or -5 according to the ACMG classification [28]. The remaining 5 SNV were of unknown functional significance (class-3). None of these variations were observed in the germline. An incidental germline mutation in the *GLA* gene was found in one case (data not shown).

Copy number variations (CNV)

Comparative genomic hybridization was used to detect amplifications and deletions. Deletions were observed in all cases. Cases 3T, 6T, 7T and 9T did not involve genes known to play a role in tumorigenesis, so are not listed in **Table 3A**. In other cases, heterozygous and homozygous deletions in known cancer-causing genes are shown in **Table 3A**. Amplifications of over 7 copies were considered as significant, as well as deletions involving more than 0.5 copy of each scored locus. Seven of 10 cases harbored amplified regions, mainly on chromosomal regions 1q21-24 (4T, 8T, 9T and 10T), 6p12 (3T), 6p21 (3T and 8T), 6q16 and 6q22-q24 (10T), 6q25-q27 (9T) and 12q13-

Table 2. Mutations analysis

Case	Signature 1	Other	TMB	Gene	Locus	Mutation	VAF
1T	82%	6 (24%)	0,73	***KIAA1549***	**7q34**	**c.2967+1G > A**	**7%**
		15 (21%)		*PAX3*	2q36.1	c.923C > T	38%
				TRAF7	16p13.3	c.1676G > T	32%
2T	29%		0,84	***BRCA2***	**13q13.1**	**c.8953+5G > A**	**17%**
3T	94%		0,94	***ARID3A***	**19p13.3**	**c.1650del**	**5%**
				CEP39	**19q13.11**	**c.499_517del**	**5%**
4T	49%	15 (45%)	0,59	***NCOR2***	**12q24.31**	**c.1494_1496dup**	**3%**
				KMT2C	7q36.1	c.2476G > T	17%
5T	86%		0,82	***TP53***	**17p13.1**	**c.473G > T**	**81%**
				ATRX	**Xq21.1**	**c.1023C > A**	**79%**
6T	-	15 (96%)	0,11				
7T	84%		0,34	*PCLO*	7q21	c.6524C > T	17%
8T	100%		0,68	***MDM2***	**12q15**	**c.1157_1158ins**	**13%**
9T	78%		1,48	***RHEB***	**7q36.1**	**c.192+2T > A**	**10%**
10T	87%		0,69	*TRIM24*	7q33.34	c.835G > T	41%

Genomic signatures were established according to Alexandrov et al. (26). TMB value is the number of variations per Megabase. In bold characters are represented class-4 and class-5 variations.

Table 3A. Genomic deletions

Case	Region	Genes
1T	**9p21.3**	***CDKN2A/2B***
	17p13	*TP53*
	17q11.2	***NF1***
	3q21-22	*GATA2*
2T	Xq23-28	*XIAP, SMARCA1, SH21A, ELF4, DUSP9, MTCP1*
4T	1q21.2	*PDE4DIP*
	19p13.3	*ARID3A, DOT1L, GADD45B, SH3GL1, STK11, TCF3…*
5T	**1q32.1**	-
	1q42.3-q44	*AKT3, FH, SMYD3*
	2q22.1	*LRP1B*
	5q33.3-34	*ITK, GABRA6*
	5q35	-
	13q14.2	***CYSLTR2, RB1, SETDB2***
	15q23	*PKM*
	17q12	-
6T	20q13	*PTPRT*
8T	13q12.11-q34	*LCP1, FOXO1, BRCA2, RB1, SERP2, FLT1/3, ZMYM2, KLF5…*
	21q22	*ERG*
10T	**1q25.3**	-
	2q22.1	***LRP1B***
	4q13.1-q13.2	*EPHA5*
	4q34.1-q34.3	*VEGFC*
	15q15.3	-
	16p11.2	*FUS, PRSS8*
	20q13	*NFATC2, PTPN1, SALL4, ZNF217*
	Xp22	*ASMTL, CRFL2, P2RY8*

Homozygous deletions are represented in bold characters.

Table 3B. Genomic amplifications over 7 copies

Case	Chromosome 1	Chromosome 6	Chromosome 12	Others
2T			***NAKA, NAB2, STAT6***	
			DDIT3, GLI1, CDK4	
			HMGA2, MDM2	
			PTPRB, FRS2	
3T		*HMGA1, CCND3*	*KMT2D, WNT1, CDK4*	2q31
		NFKBIE, HSP90AB	*MDM2, PTPRB, FRS2*	
4T	*BCL9, HIST2H3C/D*		***HDAC7, CDK4, MDM2***	16q22
	ARNT, SETDB1, FCRL4		***HMGA2, BTG1***	
	NCSTN, PRRX1, NUF2			
7T			*HMGA2, PTPRB, FRS2*	
			BTG1	
8T	*HIST2H3D*	*CCND3, CDKN1A*	*HOXC11/13,* ***SMARCC2***	3p14
		PIM1, TFEB	***CDK4, HMGA2, TBK1***	3p21
			MDM2, FRS2, ACVR1B	17p11-13
9T	*PDE4DIP,* ***SDHC***	*IGF2R, PRKN*	***B4GALNT1, CDK4***	
	FCGR2B	*AFDN, FGFR1OP*	***HMGA2, WIF1***	8q23
			MDM2, FRS2	CSMD3
10T		*SGK1*	*DDIT3, GLI1*	9q21
			B4GALNT1, CDK4	
			HMGA2, MDM2	

15 to 24-fold and ≥ 25-fold amplifications in bold and bold underlined characters respectively.

Table 4. Gene fusions

Case	Fusions	Position
3T	*ARID1B-**LIN7A***	t(6;12)(q25.3;q21.31)
5T	*DNAJC1-NEBL*	t(10;10)(p12.31;12.31)
8T	***TSPAN8**-MDM1*	t(12;12)(q21.1;q15)
	MYHAS-HOXC11	t(17;12)(p13.1;q13.13)
	SETD2-TMEM5	t(3;12)(p21.31;q14.2)
9T	*CTDSP2-CSMD3*	t(12;8)(q14.1;q23.3)
	*CSMD3-**ZFC3H1***	t(8;12)(q23.3;q21.1)
	CSMD3-DNM3OS	t(8;1)(q23.3;q24.3)
	CSMD3-PSMB1	t(8;6)(q23.3;q27)
10T	*RAP1B-**TPH2***	t(12;12)(q15;q21.1)

Genes located in 12q21 and 12q13-q15 are in bold and underlined characters respectively. All fusions are predicted to lead to a frameshift and the synthesis of a truncated protein.

q15 and 12q21-q23 encompassing *MDM2*, *CDK4* and *HGMA2* genes (all cases except 1T, 5T and 6T) (**Table 3B**).

Translocations

Five of six RNAs exhibited abnormal fusions, mainly involving regions 12q21 (2T, 8T, 9T and 10T) and 12q13-q15 (8T, 9T and 10T). Other unique fusions were observed in regions 1q24, 3p21, 6q25, 8q23, 10p12 and 17p13. Each of these fusions are predicted to lead to truncated proteins with impaired function (**Table 4**).

Methylation level

Internal and external controls showed similar methylation profiles, independently of gender, age and location of the fat tissue sample.

Four different profiles were defined: 1T, 3T, 5T and 9T exhibited hypomethylation; 4T a moderate hypermethylation, and 2T, 8T and 10T a true hypermethylation; 6T and 7T harbored a profile similar to that of normal tissues. Hypermethylation involved preferentially CpG islands and shore regions, while hypomethylation was mainly observed in shelves and out-CpG regions.

Table 5 summarizes the genetic alterations observed in the 10 DDLS tumors analyzed in the study.

Discussion

Sarcomas are a very heterogeneous group of mesenchymal malignancies, due to their large number of histological subtypes but also because of their diverse genetic classifications. For example, sarcomas can be categorized into

Table 5. Summary of genetic alterations identified in the 10 DDLS

Case	Signature 1[a]	Amplif[b]	LOH[c]	(Homozygous)	Mutation	Transloc[d]	Mitotic score[e]	Meth
6T	-	-	L	-	-	0	0-1	N
7T	++	12	L	-	-	nd	2	N
3T	++	6, 12	L	-	*ARID3A*	1	3	L
9T	++	1, 6, 8, 12	L	-	*RHEB*	4	1	L
1T	++	-	H	(*NF1*) *(CDKN2A/B)*	+	nd	1	L
5T	++	-	H	(*RB1*)	*TP53, ATRX*	1	7	L
4T	+	1, 12, 16	M	-	*NCOR2*	nd	1	M
2T	+	12	M	-	*BRCA2*	nd	9	H
8T	++	1, 6, 12	M	-	*MDM2*	3	6	H
10T	++	6, 12	H	(*LRP1B*)	-	1	8	H

Results have been sorted according to ascending methylation level: normal (N), low (L), moderate (M), high (H). [a]the signature 1 characterizing more than 50% of mutations is scored ++, 1 to 50% + and 0% -. [b]amplified regions are mentioned according the involved chromosomes; [c]the LOH level is defined as high > 5 (H), moderate [2;5] (M) and low ≤ 1 (L); [d]gives the number of translocations found in each tumor; [e]the mitotic score is evaluated as the number of mitoses observed for 10 high-power fields.

tumors with simple cytogenetic changes (one or few recurrent chromosomal alterations used in diagnostics, an example being the case of liposarcomas) or complex changes not driven by an identifiable specific genetic alteration (frequently involving common tumor suppressor genes like *TP53* or *RB* transcriptional corepressors). Sarcoma oncogenesis remains unclear for these reasons and our study was designed to focus on DDLS, a very specific and complex clinical entity, in an attempt to highlight new genetic networks.

Genomic signature, tumor mutational burden and somatic mutations

Signature 1 is reported in all types of cancer, thus it appears as not specific to a type, tissue or localization. It results from various spontaneous processes of oxidative deamination of methylated cytosines. This signature was identified in all cases but one (6T) in our study. The most frequent substitution in DDLS is therefore C > T. This signature's rate is reported to be correlated with age at diagnosis, as observed in our series, the lowest rate being found for the youngest patient 2T (**Table 2**).

Signature 15 was also observed in cases 2T, 4T and 6T. It is found mainly in gastric and small cell lung cancers, in association with a DNA-mismatch repair anomaly. Case 2T also exhibits signature 6 that can be found in 17 different types of cancer but is most common in colorectal and uterine carcinomas. This signature is also associated with a failure to repair DNA mismatches, so is mainly found in tumors with microsatellite instability [27].

The TMB, a biomarker used for therapeutic decision-making related to immunotherapy [29], was less than 1 mut/Mb in 9 cases and less than 1.5 mut/Mb in case 9T, indicating that DDLS carry a small number of mutations relative to other cancers. This might appear as contradictory in tumors with a signature related to a DNA-mismatch repair defect. However, genomic signatures have been established based on mutation types and their relative frequencies only, i.e. on a small number of mutations. Therefore, signatures 15 and 6 that were observed in 3 cases in our study might not reflect a complete defect of the DNA mismatch repair system.

Pathogenic SNVs were identified in all cases except 6T. Mutations in *TP53* (case 5T), *ATRX* (case 5T) and *PCLO* (case 7T) genes have been described in at least 5% of DDLS [7]. Mutations found in other genes were not previously reported to our knowledge. No recurrent mutation was observed, indicating that DDLS results from an accumulation of genomic events not related only to a specific initiating anomaly.

Gene amplifications

Amplified regions were detected in 7 cases. Chromosome 1 region encompassed the *HIST2H3D* gene in 2 of the 4 corresponding cases.

Similarly, the *CCND3* gene was included in the chromosome 6 amplified region in 2 of 4 cases. Amplification of a chromosome 12 region included *HGMA2* in all cases except 3T (that amplified *HGMA1*), *CDK4* and *MDM2* in all cases except 7T. Expression of *CDK4* and *MDM2* have been reported to be essential for the development of liposarcoma cell lines *in vitro*. Amplification of the 12q13-15 region might thus play a role in the initiation of liposarcoma tumorigenesis [7], suggesting a possible therapeutic benefit of *MDM2* and *CDK4* antagonists [15], presently in preclinical evaluation as well as in clinical trials.

RNA analysis revealed that fusions systematically involved amplified regions (**Tables 3B** and **4**): i) the 12q13-15 and 12q21 regions are amplified in 6 of 7 cases; ii) the 17p13.1 and 3p21.31 regions are amplified in case 8T; iii) the *TSPAN8-MDM1* (case 8T) and *RAP1B-TPH2* (case 10T) fusions associate the 12q15 and 12q21 regions, i.e. the two most frequently amplified regions; iv) finally, four fusions were detected in case 9T, all involving the *CSMD3* gene located in 8q23.3, amplified in this tumor and fused with the 12q14.1, 12q21.1, 1q24.3 and 6q27 regions, also amplified in this tumor. This gene is known to be involved in dendritic cell development and has not previously been described to play a role in the development of DDLS [30].

A recent study on liposarcoma reported a detailed characterization of observed fusions including the corresponding genes and their putative functional consequences [7]. However, we observed several translocations in each amplified region, some involving genes not known to have a specific role in tumorigenesis (*CSMD3* as an example). This observation does not suggest a specific causative link. Although recurrent translocations have been described as pivotal in certain tumor processes, including sarcomas, the translocations observed in this study of DDLS are neither recurrent nor specific. Therefore, they seem more likely to play a role in initiation of the amplification process rather than having a specific functional role in the tumorigenesis of DDLS. This hypothesis has also been studied by Bianchi et al. [31] who reported it as a rare event in a poorly differentiated synovial sarcoma [32]. On the contrary, amplifications promoted by prior fusions seem to be a frequent mechanism in DDLS. In contrast, case 5T exhibits a unique translocation of chromosome 10, probably an inversion, responsible for premature disruption of the *NEBL* gene's reading frame.

Loss of heterozygosity

Three different levels of LOH were noticed: high in cases 1T, 5T, 10T, moderate in 2T, 4T, 8T and low in 3T, 6T, 7T, 9T (**Table 3A**). Recurrent LOHs have been reported in DDLS including the *NF1* (28%), *CDKN2A* and *CDKN2B* (44%) genes [8]. In our series, *NF1* was lost in cases 1T and 5T, and *CDKN2A/CDKN2B* in cases 1T, 5T and 10T. Case 1T harbored a homozygous deletion of these 3 tumor suppressor genes. *RB1* and *BRCA2* LOH have also been found in 60% of DDLS [33]. They were lost in cases 1T, 2T, 5T and 8T. In case 5T, both alleles of the *RB1* gene were deleted, and inactivation of the *BRCA2* gene by mutation and deletion was observed in case 2T. Finally, case 4T presented a single interstitial LOH on chromosome 19p, including several genes such as *STK11* and *ARID3A*. A mutation of *ARID3A* was also observed in case 3T. All these genes, in addition to frequent somatic mutations in various types of cancers, are involved in cancer predisposition when mutated in the germ line. The pRB protein has been identified as playing a role in the dedifferentiation of LPS via *RB1* gene alteration or interaction with *CDK4* and *MDM2*. In the same way, pRB has been shown to promote adipocyte differentiation by increasing DNA binding by C/EBPβ transactivation and/or by inhibiting Ras signaling [33], thus identifying another potential route to develop targeted therapy.

Methylation level

Methylation variations appear to be independent of age, sex and tumor location. However, hypermethylated tumors have a greater tendency to proliferate than hypomethylated tumors (**Table 5**). Furthermore, tumors can be divided in 3 groups: i) hypomethylation amplifications (cases 3T, 9T and 7T); ii) hypomethylation and LOH (cases 1T and 5T); iii) hypermethylation, amplifications and LOH (cases 4T, 2T, 8T and 10T). No specificity was observed related to the clinical issue of patients.

Case 6T did not show any mutation or amplification, and a unique interstitial LOH of the

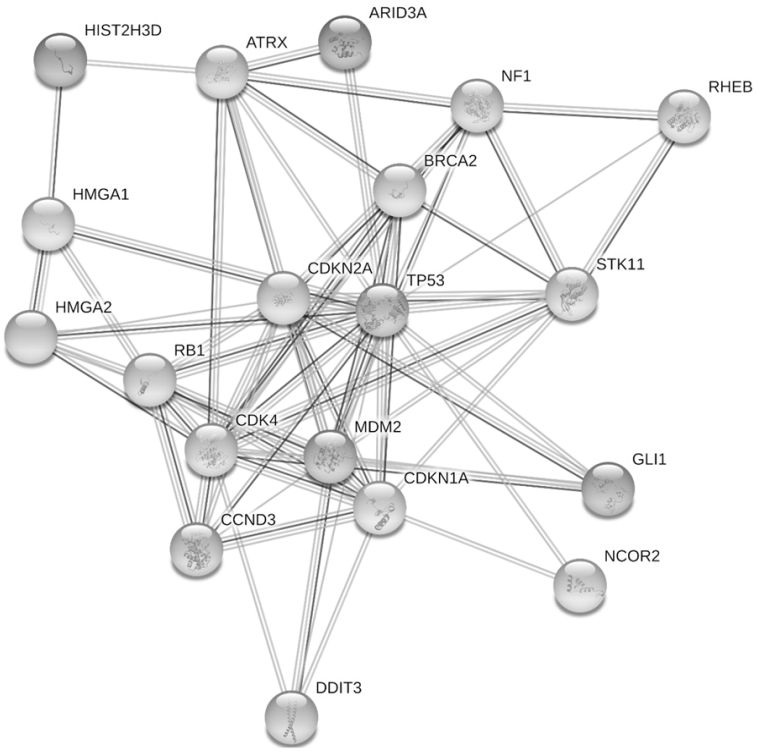

Figure 1. STRING interactions of proteins altered in DDLS. All proteins showing an alteration in the series of 10 DDLS were entered in a STRING request that returned a homogeneous network focused on p53 control.

20q13 region. This region contains the *PTPRT* gene, tyrosine phosphatase from the Rho family of proteins, recently described as mutated in several types of cancer [34]. Clinically, it was the only case diagnosed at a very early stage, with no necrosis, no active proliferation, no recurrence after surgical treatment. This observation reinforces the previous reports of genetically stable tumors as being less clinically aggressive [35-38].

Our work did not reveal any specific genetic alteration linked to clinical outcomes, although this may be due to the small number of patients enrolled in this series. Furthermore, we cannot exclude a role of the microenvironment besides the usually aggressive behavior of dedifferentiated sarcomas.

In summary, this study showed that DDLS exhibits a diverse pattern of genomic and methylation profiles. Amplification is the most frequent alteration, that probably occurs consecutively to chromosome fusions. Cases 1T and 5T did not harbor amplifications but instead numerous deletions and mutations of tumor suppressor genes, which could be an alternative mechanism of tumorigenesis. From these observations, therapeutic hypotheses can be considered. The most frequent anomaly is the amplification of chromosome 12, involving the *CDK4*, *MDM2* and/or *HMGA2* genes, *MDM2* and *HMGA2* showing the highest levels of amplification. Suppression of *HMGA2* by antisense RNAs could thus be tested in vitro as a potential target for DDLS. In atypical lipomatous tumors, this treatment is able to inhibit cell growth *in vitro* and to induce apoptosis in neoplastic cells overexpressing *HMGA2* [39]. Inhibition of *MDM2* could also be considered by targeting the pathway of proteasome degradation by ubiquitination in order to maintain normal p53 activity [40]. These observations converge on the hypothesis that deregulation of the p53 protein appears to be the key element controlling proliferation in DDLS (**Figure 1**). The different amplifications overactivate mechanisms blocking the normal functions of p53, such as its degradation in the proteasome *via* MDM2-mediated ubiquitination and cell growth mediated by *CDK4* and *HMGA2*. The LOHs in combination with somatic mutations contribute to inactivate tumor suppressor genes (*NF1*, *RB1*, *BRCA2*, *CDKN2A*) also involved in p53 regulation. To reinforce this primary hypothesis on a recurrent indirect mechanism of p53 inactivation in DDLS tumorigenesis, we are currently elaborating on defining a biomathematics model of genetic interactions. This model would help to understand the many biological processes and identify the best targets which would be able to modify the network and could be further tested in *in vitro* models. This model also might allow insight into the mechanisms of tumorigenesis in Li-Fraumeni syndrome, associated with germline *TP53* mutations and a high predisposition to cancers including sarcomas.

Acknowledgements

This work was funded by Ramsay santé and PIGeOn SAS. We are grateful to Dr Valérie DELAGUE and her team, who participated to the experimental procedures. We also thank Integragen France for its constant availability and appreciable reactivity during this confusing period. This work was funded by Ramsay santé and PIGeOn SAS.

Disclosure of conflict of interest

None.

Address correspondence to: Sylviane Olschwang, INSERM UMR1251 Marseille Medical Genetics, Faculté de Médecine Timone, 27 boulevard Jean Moulin, 13005 MARSEILLE France. Tel: +33(0)608 810 017; E-mail: sylviane.olschwang@inserm.fr

References

[1] Fletcher CD. The evolving classification of soft tissue tumours-an update based on the new 2013 WHO classification. Histopathology 2014; 64: 2-11.

[2] Coindre JM, Pédeutour F and Aurais A. Well-differentiated and dedifferentiated liposarcomas. Virchows Archiv 2010; 456: 167-179.

[3] Johnson CN, Ha AS, Chen E and Davidson D. Lipomatous soft-tissue tumors. J Am Acad Orthop Surg 2018; 26:779-788.

[4] Rais G, Andaloussi MB, Raissouni S, Barki A, Allaoui M, Zouaidia F, Afif M, Mrabti H and Errihani H. Dedifferentiated liposarcoma of the spermatic cord: therapeutic difficulties of large tumors. Pan Afr Med J 2011; 8: 49.

[5] Ferrari A, Dirksen U and Bielack S. Sarcomas of soft tissue and bone. Prog Tumor Res 2016; 43: 128-141.

[6] Terrier P. Liposarcomas. Ann Pathol 2012; 32: S108-110.

[7] Hirata M, Asano N, Katayama K, Yoshida A, Tsuda Y, Sekimizu M, Mitani S, Kobayashi E, Komiyama M, Fujimoto H, Goto T, Iwamoto Y, Naka N, Iwata S, Nishida Y, Hiruma T, Hiraga H, Kawano H, Motoi T, Oda Y, Matsubara D, Fujita M, Shibata T, Nakagawa H, Nakayama R, Kondo T, Imoto S, Miyano S, Kawai A, Yamaguchi R, Ichikawa H and Matsuda K. Integrated exome and RNA sequencing of dedifferentiated liposarcoma. Nat Commun 2019; 10: 1-12.

[8] Cancer Genome Atlas Research Network. Comprehensive and integrated genomic characterization of adult soft tissue sarcomas. Cell 2017; 171: 950-965.

[9] Amer KM, Congiusta DV, Thomson JE, Elsamna S, Chaudhry I, Bozzo A, Amer R, Siracuse B, Ghert M and Beebe KS. Epidemiology and survival of liposarcoma and its subtypes: a dual database analysis. J Clin Orthop Trauma 2020; 11: S479-S484.

[10] Knebel C, Lenze U, Pohlig F, Lenze F, Harrasser N, Suren C, Breitenbach J, Rechl H, von Eisenhart-Rothe R and Mühlhofer HML. Prognostic factors and outcome of liposarcoma patients: a retrospective evaluation over 15 years. BMC Cancer 2017; 17: 410.

[11] Gundle KR, Kafchinski L, Gupta S, Griffin AM, Dickson BC, Chung PW, Catton CN, O'Sullivan B, Wunder JS and Ferguson PC. Analysis of margin classification systems for assessing the risk of local recurrence after soft tissue sarcoma resection. J Clin Oncol 2018; 36: 704-719.

[12] Chibon F, Lagarde P, Salas S, Pérot G, Brouste V, Tirode F, Lucchesi C, de Reynies A, Kauffmann A, Bui B, Terrier P, Bonvalot S, Le Cesne A, Vince-Ranchère D, Blay JY, Collin F, Guillou L, Leroux A, Coindre JM and Aurias A. Validated prediction of clinical outcome in sarcomas and multiple types of cancer on the basis of a gene expression signature related to genome complexity. Nat Med 2010; 16: 781-787.

[13] Ray-Coquard I, Serre D, Reichardt P, Martín-Broto J and Bauer S. Options for treating different soft tissue sarcoma subtypes. Future Oncol 2018; 14: 25-49.

[14] Mattei JC, Bouvier-Labit C, Barets D, Macagno N, Chocry M, Chibon F, Morando P, Rochwerger RA, Duffaud F, Olschwang S, Salas S and Jiguet-Jiglaire C. Pan aurora kinase inhibitor: a promising targeted-therapy in dedifferentiated liposarcomas with differential efficiency depending on sarcoma molecular profile. Cancers (Basel) 2020; 12: 583.

[15] Conyers R, Young S and Thomas DM. Liposarcoma: molecular genetics and therapeutics. Sarcoma 2011; 2011: 483154.

[16] Lee ATJ, Thway K, Huang PH and Jones RL. Clinical and molecular spectrum of liposarcoma. J Clin Oncol 2018; 36: 151-159.

[17] Weber M. P Profiles of DNA methylation in normal and cancer cells. Med Sci (Paris) 2008; 24: 731-734.

[18] Deltour S, Chopin V and Leprince D. Epigenetics and cancer. Med Sci (Paris) 2005; 21: 405-411.

[19] Weber M, Davies JJ, Wittig D, Oakeley EJ, Haase M, Lam WL and Schübeler D. Chromosome-wide and promoter-specific analyses identify sites of differential DNA methylation in normal and transformed human cells. Nat Genet 2005; 37: 853-862.

[20] Shann YJ, Cheng C, Chiao CH, Chen DT, Li PH and Hsu MT. Genome-wide mapping and characterization of hypomethylated sites in human tissues and breast cancer cell lines. Genome Res 2008; 18: 791-801.

[21] Tombolan L, Poli E, Martini P, Zin A, Millino C, Pacchioni B, Celegato B, Bisogno G, Romualdi C, Rosolen A and Lanfranchi G. Global DNA methylation profiling uncovers distinct methylation patterns of protocadherin alpha4 in metastatic and non-metastatic rhabdomyosarcoma. BMC Cancer 2016; 16: 886.

[22] Rello-Varona S and Tirado OM. DNA methylation profiling opens a new phase in the search of targeted therapy against Ewing sarcoma. Pharmacogenomics 2017; 18: 1307-1309.

[23] Zhang W, Han S and Sun K. Combined analysis of gene expression, miRNA expression and DNA methylation profiles of osteosarcoma. Oncol Rep 2017; 37: 1175-1181.

[24] Gnirke A, Melnikov A, Maguire J, Rogov P, LeProust EM, Brockman W, Fennell T, Giannoukos G, Fisher S, Russ C, Gabriel S, Jaffe DB, Lander ES and Nusbaum C. Solution hybrid selection with ultra-long oligonucleotides for massively parallel targeted sequencing. Nat Biotechnol 2009; 27: 182-189.

[25] Lawrence MS, Stojanov P, Polak P, Kryukov GV, Cibulskis K, Sivachenko A, Carter SL, Stewart C, Mermel CH, Roberts SA, Kiezun A, Hammerman PS, McKenna A, Drier Y, Zou L, Ramos AH, Pugh TJ, Stransky N, Helman E, Kim J, Sougnez C, Ambrogio L, Nickerson E, Shefler E, Cortés ML, Auclair D, Saksena G, Voet D, Noble M, DiCara D, Lin P, Lichtenstein L, Heiman DI, Fennell T, Imielinski M, Hernandez B, Hodis E, Baca S, Dulak AM, Lohr J, Landau DA, Wu CJ, Melendez-Zajgla J, Hidalgo-Miranda A, Koren A, McCarroll SA, Mora J, Crompton B, Onofrio R, Parkin M, Winckler W, Ardlie K, Gabriel SB, Roberts CWM, Biegel JA, Stegmaier K, Bass AJ, Garraway LA, Meyerson M, Golub TR, Gordenin DA, Sunyaev S, Lander ES and Getz G. Mutational heterogeneity in cancer and the search for new cancer-associated genes. Nature 2013; 499: 214-218.

[26] Niu B, Ye K, Zhang Q, Lu C, Xie M, McLellan MD and Ding L. MSIsensor: microsatellite instability detection using paired tumor-normal sequence data. Bioinformatics 2014; 30: 1015-1016.

[27] Alexandrov LB, Kim J, Haradhvala NJ, Huang MN, Tian Ng AW, Wu Y, Boot A, Covington KR, Gordenin DA, Bergstrom EN, Islam SMA, Lopez-Bigas N, Klimczak LJ, McPherson JR, Morganella S, Sabarinathan R, Wheeler DA and Mustonen V; PCAWG Mutational Signatures Working Group, Getz G, Rozen SG and Stratton MR; PCAWG Consortium. The repertoire of mutational signatures in human cancer. Nature 2020; 578: 94-101.

[28] Richards S, Aziz N, Bale S, Bick D, Das S, Gastier-Foster J, Grody WW, Hegde M, Lyon E, Spector E, Voelkerding K and Rehm HL. Standards and guidelines for the interpretation of sequence variants: a joint consensus recommendation of the American college of medical genetics and genomics and the association for molecular pathology. Genet Med 2015; 17: 405-424.

[29] McNamara MG, Jacobs T, Lamarca A, Hubner RA, Valle JW and Amir E. Impact of high tumor mutational burden in solid tumors and challenges for biomarker application. Cancer Treat Rev 2020; 89: 102084.

[30] Somaiah N, Beird HC, Barbo A, Song J, Mills Shaw KR, Wang WL, Eterovic K, Chen K, Lazar A, Conley AP, Ravi V, Hwu P, Futreal A, Simon G, Meric-Bernstam F and Hong D. Targeted next generation sequencing of well-differentiated/dedifferentiated liposarcoma reveals novel gene amplifications and mutations. Oncotarget 2018; 9: 19891-19899.

[31] Bianchi JJ, Murigneux V, Bedora-Faure M, Lescale C and Deriano L. Breakage-fusion-bridge events trigger complex genome rearrangements and amplifications in developmentally arrested T cell lymphomas. Cell Rep 2019; 27: 2847-2858, e4.

[32] Di Mauro I, Mescam-Mancini L, Chetaille B, Lae M, Pierron G, Dadone-Montaudie B, Bazin A, Bouvier C, Michiels JF and Pedeutour F. MDM2 amplification and fusion gene ss18-ssx in a poorly differentiated synovial sarcoma: a rare but puzzling conjunction. Neoplasia 2020; 22: 311-321.

[33] Takahira T, Oda Y, Tamiya S, Yamamoto H, Kobayashi C, Izumi T, Ito K, Iwamoto Y and Tsuneyoshi M. Alterations of the RB1 gene in dedifferentiated liposarcoma. Mod Pathol 2005; 18: 1461-1470.

[34] Yu J, Becka S, Zhang P, Zhang X, Brady-Kalnay SM and Wang Z. Tumor-derived extracellular mutations of PTPRT/PTPρ are deficient in cell adhesion. Mol Cancer Res 2008; 6: 1106-1113.

[35] Takahashi H, Asaoka M, Yan L, Rashid OM, Oshi M, Ishikawa T, Nagahashi M and Takabe K. Biologically aggressive phenotype and anticancer immunity counterbalance in breast cancer with high mutation rate. Sci Rep 2020; 10: 1852.

[36] Bui NQ, Przybyl J, Trabucco SE, Frampton G, Hastie T, van de Rijn M and Ganjoo KN. A clinico-genomic analysis of soft tissue sarcoma patients reveals CDKN2A deletion as a biomarker for poor prognosis. Clin Sarcoma Res 2019; 9: 12.

[37] Taylor BS, Barretina J, Maki RG, Antonescu CR, Singer S and Ladanyi M. Advances in sarcoma genomics and new therapeutic targets. Nat Rev Cancer 2011; 11: 541-557.

[38] Carbonnaux M, Brahmi M, Schiffler C, Meeus P, Sunyach M-P, Bouhamama A, Karanian M, Tirode F, Pissaloux D, Vaz G, Ray-Coquard I, Blay JY and Dufresne A. Very long-term survivors among patients with metastatic soft tissue sarcoma. Cancer Med 2019; 8: 1368-1378.

[39] Pentimalli F, Dentice M, Fedele M, Pierantoni GM, Cito L, Pallante P, Santoro M, Viglietto G, Dal Cin P and Fusco A. Suppression of HMGA2 protein synthesis could be a tool for the therapy of well differentiated liposarcomas overexpressing HMGA2. Cancer Res 2003; 63: 7423-7427.

[40] Halasi M, Pandit B and Gartel AL. Proteasome inhibitors suppress the protein expression of mutant p53. Cell Cycle 2014; 13: 3202-3206.